Proprietary Information
Withhold from Public Disclosure Under 10 CFR 2.390
This letter is decontrolled when separated from Enclosure 1

Tennessee Valley Authority, 1101 Market Street, Chattanooga, Tennessee 37402

CNL-16-117

July 29, 2016

10 CFR 50.90

ATTN: Document Control Desk
U.S. Nuclear Regulatory Commission
Washington, D.C. 20555-0001

Browns Ferry Nuclear Plant, Units 1, 2, and 3
Renewed Facility Operating License Nos. DPR-33, DPR-52, and DPR-68
NRC Docket Nos. 50-259, 50-260, and 50-296

Subject: **Proposed Technical Specifications (TS) Change TS-505 - Request for License Amendments - Extended Power Uprate (EPU) - Supplement 26, Responses to Requests for Additional Information**

References: 1. Letter from TVA to NRC, CNL-15-169, "Proposed Technical Specifications (TS) Change TS-505 - Request for License Amendments - Extended Power Uprate (EPU)," dated September 21, 2015 (ML15282A152)

2. Letter from NRC to TVA, "Browns Ferry Nuclear Plant, Units 1, 2, and 3 - Request for Additional Information Related to License Amendment Request Regarding Extended Power Uprate (CAC Nos. MF6741, MF6742, and MF6743)," dated June 3, 2016 (ML16144A643)

By the Reference 1 letter, Tennessee Valley Authority (TVA) submitted a license amendment request (LAR) for the Extended Power Uprate (EPU) of Browns Ferry Nuclear Plant (BFN) Units 1, 2 and 3. The proposed LAR modifies the renewed operating licenses to increase the maximum authorized core thermal power level from the current licensed thermal power of 3458 megawatts to 3952 megawatts. The Reference 2 letter provided Nuclear Regulatory Commission (NRC) Requests for Additional Information (RAIs) related to the replacement steam dryers. The due date, provided by the Reference 2 letter, for the responses to NRC RAIs EMCB-RAIs 1, 4, 5, 6, 7, 8, 12, 20, 23, 25, 28, 33, 35, 38, 39, 40, 41, 42, and 43 is July 29, 2016.

Enclosure 1 to this letter provides the responses to NRC RAIs EMCB-RAIs 1, 4, 5, 6, 7, 8, 12, 20, 23, 25, 28, 33, 35, 38, 39, 40, 41, 42, and 43. GE-Hitachi Nuclear Energy Americas LLC (GEH) considers portions of the information provided in Enclosure 1 of this letter to be proprietary and, therefore, exempt from public disclosure pursuant to 10 CFR 2.390, Public inspections, exemptions, requests for withholding. An affidavit for withholding information, executed by GEH, is provided in Enclosure 3. Enclosure 2 to this letter provides a non-proprietary version of the responses to the RAIs provided in Enclosure 1. Therefore, on behalf of GEH, TVA requests that Enclosure 1 be withheld from public disclosure in accordance with the GEH affidavit and the provisions of 10 CFR 2.390.

TVA has reviewed the information supporting a finding of no significant hazards consideration and the environmental consideration provided to the NRC in the Reference 1 letter. The supplemental information provided in this submittal does not affect the bases for concluding that the proposed license amendment does not involve a significant hazards consideration. In addition, the supplemental information in this submittal does not affect the bases for concluding that neither an environmental impact statement nor an environmental assessment needs to be prepared in connection with the proposed license amendment. Additionally, in accordance with 10 CFR 50.91(b)(1), TVA is sending a copy of this letter to the Alabama State Department of Public Health.

There are no new regulatory commitments associated with this submittal. If there are any questions or if additional information is needed, please contact Edward D. Schrull at (423)751-3850.

I declare under penalty of perjury that the foregoing is true and correct. Executed on the 29th day of July 2016.

Respectfully,

J. W. Shea
Vice President, Nuclear Licensing

Enclosures:

1. Responses to NRC Requests for Additional Information EMCB-RAIs 1, 4, 5, 6, 7, 8, 12, 20, 23, 25, 28, 33, 35, 38, 39, 40, 41, 42, and 43 (Proprietary version)
2. Responses to NRC Requests for Additional Information EMCB-RAIs 1, 4, 5, 6, 7, 8, 12, 20, 23, 25, 28, 33, 35, 38, 39, 40, 41, 42, and 43 (Non-proprietary version)
3. General Electric Hitachi Affidavit

cc:

NRC Regional Administrator - Region II
NRC Senior Resident Inspector - Browns Ferry Nuclear Plant
State Health Officer, Alabama Department of Public Health (w/o Enclosure 1)

Withhold from Public Disclosure Under 10 CFR 2.390

ENCLOSURE 1
Responses to NRC Requests for Additional Information
EMCB-RAIs 1, 4, 5, 6, 7, 8, 12, 20, 23, 25, 28, 33, 35, 38, 39, 40, 41, 42, and 43

(Proprietary version)

ENCLOSURE 2
Responses to NRC Requests for Additional Information
EMCB-RAIs 1, 4, 5, 6, 7, 8, 12, 20, 23, 25, 28, 33, 35, 38, 39, 40, 41, 42, and 43

(Non-proprietary version)

EMCB-RAI 1

In Section 3.2.2.2 of NEDC-33824P (Reference 6), the licensee discusses the design improvements made in the BFN RSDs to increase fatigue margins.

a. Describe the types of welds introduced by these improvements.

b. Describe if any of these welds connect more than two components and have heat-affected zones that may be susceptible to fatigue cracking.

c. Also discuss if any of these welds require testing of the weld samples.

d. Address if these welds receive solution heat treatment or annealing.

GEH Response

a. Weld types introduced by the design improvements detailed in Section 3.2.2.2 are given in the table below:

SDAR Improvement Listing Order	Improvement Description	Types of Welds Introduced
1	One Piece Tie Bars	No new Types
2	One Piece Top Caps	Type II
3	Drain Pipe Flange Addition	Type I
4	Hood Support Stiffeners Addition	Type III
5	Outlet End Plate Segmentation for Access	Type I
6	Center Outlet End Plate Thicker / C-Channel Support	Type III
7	Center Bank Support Plates added	Type I
8	Outlet End Plate Scallop Deepening	No new Types
9	Trough Plate Modifications	Type II
10	Condensate Drain Slot Shortened	No new Types
11	Drain Channel Plates Thickened	No new Types
12	Drain Channel Azimuthal Span Shortened	No new Types
13,14	Skirt Drain Channel Improvements	Type I, III
15,16	Skirt Tabs and Lower Ring Improvements	Type I, III

ASME BPVC Section III Subsection NG Weld Types:
Type I – Complete joint penetration welds between plates in same plane
Type II – Complete joint penetration welds between plates with integral backing
Type III – Complete joint penetration welds between plates that have joint angles up to 90°
Type IV – Partial joint penetration welds of double groove design
Type V – Double fillets or groove welds with supporting fillets on the opposite side
Type VI – Partial penetration welds of single groove design
Type VII – Single fillet welds
Type VIII – Intermittent fillet or plug welds

Note: The weld types added as part of the improvements were all complete penetration welds and do not include all the dryer weld types listed.

b. Added welds that connect more than two components in areas of fatigue concern are as follows:

1. Hood support stiffeners

2. Upper attachment point of the C-channel support (as part of the improved center outlet end plate)
3. Trough end-bank attachments

The added hood support stiffeners (Figures 1-1 and 1-2) drive some of the hood support load into the trough base plates (diverting some load from the common point where the hood support, trough side plate, and trough base plates all come together) thereby addressing fatigue cracking that has occurred at this location in curved hood dryers. The thicker center outlet end plate and C-channel (Figure 1-3) help drive the frequency outside the SRV resonant frequency thereby reducing stress and fatigue susceptibility in these areas. The trough plate modifications (Figure 1-4) eliminated many partial penetration welds thereby improving the fatigue performance of these joints.

Fatigue stresses in austenitic stainless steels are influenced by the weld geometry and not weld microstructure. The heat affected zones associated with these welds will have fatigue performance similar to that of the weld metal in the steam dryer.

c. The trough plate modification and top cap improvements both introduced Type II joints which cannot be inspected from the backside in production.

   As stated in NEDC-33824P Appendix A, Section 4.3; where the root side of the weld cannot be inspected, such as fillet welds and partial penetration welds, or full penetration welds with backing, robust weld process qualifications are conducted to prevent weld defects from occurring during fabrication. A representative sample (mock-up) of the trough plate and top cap welds (using the same joint design and material types) will be destructively tested. Metallurgical evaluations will be conducted to demonstrate an acceptable weld root prior to weld procedure approval.

   Mechanical property testing requirements (e.g., tensile and bend tests) for the welds in the table above only involve those required for weld procedure qualification per American Society of Mechanical Engineers (ASME) Boiler and Pressure Vessel Code (BPVC) Section IX.

d. The trough sub-assemblies are given a post-weld solution treatment prior to incorporation into the larger bank assemblies. All of the other weld improvements affect larger steam dryer assemblies that are not practical to solution heat treat. As a result, the trough end bank attachments are the only weld improvements listed above that undergo a post-weld solution heat treatment.

[[

]]

Figure 1-1. Hood Support Stiffener (Common T Side View with Trough Removed)

[[

]]

Figure 1-2. Hood Support Stiffener (Section View from Trough)

[[

]]

Figure 1-3. C-Channel Upper Attachment Location

[[

]]

Figure 1-4. Trough Extension Attachment Location

Changes to NEDC-33824P Revision 0 – BFN Steam Dryer Analysis Report (SDAR):

None

EMCB-RAI 4

Section 5.1.1 (page 5-1 of Reference 6) lists the materials used in the manufacture of the steam dryer assembly: [[

]]. Provide information on the heat treatment and fabrication techniques employed for the RSDs to improve resistance to Intergranular Stress Corrosion cracking (IGSCC) and fatigue cracking. Address the following items.

a. Describe whether there are any areas of the RSDs with crevices. If there are any, please provide the locations and their impact on IGSCC, and the corresponding alternating stress ratios (ASRs).

b. Describe any measures implemented in the fabrication of the RSDs to minimize residual stresses.

c. Describe the solution annealing or other heat treatments applied to the materials prior to and subsequent to manufacturing.

d. Describe whether any cold forming is introduced during fabrication. In case cold forming is introduced, discuss any mitigation measures.

GEH Response

a. While crevices have been eliminated to the extent possible by complete joint penetration welds and sealing of potential creviced areas, some locations can be considered potential crevices. The creviced locations which are stainless steel are in the [[

]]. The fabrication of the dryer uses solution annealed low carbon stainless steel (C≤0.020%) for the dryer (which prevents sensitization as a result of welding) to reduce the risk of Intergranular Stress Corrosion Cracking (IGSCC) at these locations. It should be noted that IGSCC associated with crevices has not been reported in the original operating plant dryers, which were fabricated from Type 304 stainless steel with a maximum carbon content of 0.08%.

The locations of creviced components and alternating stress ratios (ASRs) are as follows:

Weld	Alternating Stress Ratio
[[	

Weld	Alternating Stress Ratio
	]]

[[

]]

Where specifically analyzed, all of the subject locations have ASR values above the required value of 2. [[

]]

b. The methods used to reduce residual stress are in accordance with the requirements of Boiling Water Reactor Vessel and Internals Project (BWRVIP)-84 (Reference 4-1) and BWRVIP-181-A (Reference 4-2). Residual stresses in the dryer components are addressed in several ways: (1) where practical, welded assemblies (e.g., the dryer support ring) are solution heat treated subsequent to welding; (2) cold forming operations are followed by solution heat treatment if the forming operation exceeds 2.5% plastic strain; (3) controlled grinding and polishing of weld and weld heat affected zones is used to reduce the surface residual stresses;(4) weld pass thickness is controlled, which reduces the heat input inducing less residual stress into the surrounding structure and less weld residual stress from weld shrinkage; (5) weld layer sequencing is used to control distortion thereby reducing the need for post weld straightening; and (6) alignment and gap between members to be welded is controlled to minimize weld metal volume used in the weld joint thereby reducing residual stress.

c. Raw material: Solution heat treatment (and aging for Alloy X-750) of the raw materials will be performed in accordance with the requirements of the material specifications (e.g., SA-240) and the additional GE Hitachi Nuclear Energy (GEH) requirements as follows:

300 series stainless steel: Material will be heat treated at 1,900-2,100°F (bulk metal temperature) for 15 minutes per inch of thickness, but not less than 15 minutes, immediately followed by a water quench.

Alloy X-750: Material will be heat treated at 1,975–2,025°F for 60-70 minutes, followed by cooling below 1,100°F within 10 minutes. Re-heated and age hardened at 1,300±25°F for 20-21 hours, followed by air cooling.

Fabrication: Solution heat treatment performed as part of fabrication activities on 300 series stainless steel will be performed in one of two ways: (1) same method as the raw material; or (2) vacuum solution anneal at 1,900-2,100°F (bulk metal temperature) for 15 minutes per inch of thickness, but not less than 15 minutes, immediately followed by a nitrogen or argon gas quench.

It should also be noted that all material will be tested subsequent to solution annealing in accordance with American Society for Testing and Materials (ASTM) A262 Practice E (Reference 4-3).

d. Cold forming is required for some of the dryer components. GEH imposes a limit of 2.5% permanent plastic strain for forming operations during fabrication, which includes standard processes such as straightening operations. For those components where the forming operation results in a strain greater than 2.5%, solution annealing, as described in Part c, above, is performed subsequent to the cold forming operation.

References:

4-1. BWRVIP-84, Revision 2-A, "BWR Vessel and Internals Project, Guidelines for Selection and Use of Materials for Repairs to BWR Internal Components," EPRI Technical Report 3002007385, March 2016.

4-2. BWRVIP-181-A, "BWR Vessel and Internals Project, Steam Dryer Repair Design Criteria," EPRI Technical Report 1020997, October 2010.

4-3. ASTM A262, "Standard Practices for Detecting Susceptibility to Intergranular Attack in Austenitic Stainless Steels," 2015.

Changes to NEDC-33824P Revision 0 – BFN Steam Dryer Analysis Report (SDAR):

None

EMCB-RAI 5

Confirm that the weld pass thickness, which is discussed in Section 4.2 of NEDC-33824P, Appendix A (Reference 8), will be smaller than the critical flaw size. In addition, the licensee is requested to have a requirement that the root and final passes of dryer welds are inspected using a liquid penetrant test during the fabrication of the replacement steam dryers for the three Browns Ferry Units.

GEH Response

In response to EMCB-RAI 5, a fracture mechanics analysis was performed on critical weld locations demonstrating that proposed weld pass thicknesses would not result in flaws for which the peak-to-peak stress intensity factor would exceed the fatigue crack growth threshold of the replacement steam dryer stainless steel. Various joint configurations and weld pass thicknesses were considered in the evaluation. Weld locations were chosen for evaluation at both high Flow-Induced Vibration (FIV) fatigue stress locations (i.e., [[ ]]) and high FIV [[ ]] stress locations (i.e., [[ ]]). Postulated flaws at all locations were shown to have [[ ]] of the material. Therefore, weld pass thicknesses are demonstrated to be less than the critical flaw size. Details of the analysis and weld pass thickness are discussed as follows.

The Browns Ferry Nuclear Plant (BFN) replacement steam dryers weld pass size will vary up to [[ ]] thick. The pass thickness depends on the thickness of the members to be welded and the welding process used, for example a joint [[ ]] thick will not be welded in [[ ]], however a [[ ]] thick joint may have passes up to [[ ]] thick on the fill and final weld passes. Due to fabrication root layer requirements, the weld root will not have a pass greater than [[ ]] thick, but the weld toe located at the weld face may have a weld pass up to [[ ]] thick.

Fatigue cracks are known to initiate on the surface. The fabrication process of the replacement steam dryer will utilize Non-Destructive Examination (NDE) methods to ensure no surface flaws exist that could result in fatigue crack growth. As discussed in NEDC-33824P Section 4.2.3.5.1 and Appendix A Section 4.3, the root and final passes of all [[ ]] welds will be inspected using liquid penetrant testing. In conjunction with these NDE examination techniques, weld processes will be qualified to prevent defects from occurring. Qualified weld processes will include, as necessary for [[ ]]. These NDE methods and weld joint qualifications will limit the occurrence of weld surface flaws.

The final Extended Power Uprate (EPU) FIV stress results ([[ ]]), generated in the development of NEDC-33824P, were used to select locations for the peak-to-

peak stress intensification factor calculations. Table 5-1 summarizes the locations considered in this evaluation as well as fracture mechanics analysis results for each postulated [[ ]] flaw.

Table 5-1: Limiting Components Based on FIV Fatigue Stress at EPU

Weld	Adjusted Stress (psi)	Weld Throat Minimum (in)	Weld Type[3]	Weld Pass Thickness Limit (in)	Assumed [[ ]] Flaw Size ([[ ]]) (in)	ΔK_I (ksi-√in)	Fatigue Crack Growth (FCG) Threshold (ksi-√in)	Critical Flaw ΔK_I < FCG Threshold?
[[								
								]]

Notes:

1. [[ ]]
2. [[ ]]; no Mode I crack opening.
3. CJP is complete joint penetration, PJP is partial joint penetration.

The weld location with the maximum alternating stress intensity at EPU conditions, determined based on the lowest Minimum Alternating Stress Ratio (MASR), is the [[ ]] weld. The [[ ]] weld is a [[ ]]. In order to address the different types of welds used in the dryer fabrication, the location with the lowest MASR in a [[ ]] were also examined. These locations are the connection between the [[ ]], respectively. Table 5-1 also considers the [[ ]]. Additionally, proposed weld bead sizes were evaluated for other high stress and high [[ ]] stress locations to confirm conclusions that postulated flaws, equal in size to the weld bead, would not result in fatigue crack growth. Based on the consideration of the (1) highest stressed weld locations, (2) multiple joint configurations, and (3) the largest flaws as a percentage of thickness these fracture mechanics results will [[ ]].

Despite conservative assumptions regarding flaw size and postulation of flaws at the highest stressed welds in the dryer, the Table 5-1 fracture mechanics analysis results show that the calculated [[ ]] of the postulated weld flaws are less than the fatigue crack growth threshold value of [[ ]] (Reference 5-1).

This assessment confirms that a [[ ]] weld flaw would be unlikely to grow by fatigue when subjected to the maximum alternating stress intensity under EPU loading conditions and that the weld pass thickness is smaller than the critical flaw size for all locations on the dryer.

Reference:

5-1. Rolfe, S.T. and Barsom, J.M., Fracture and Fatigue Control in Structures – Application of Fracture Mechanics, pages 224 and 225, Prentice-Hall Inc., 1977.

Changes to NEDC-33824P Revision 0 – BFN Steam Dryer Analysis Report (SDAR):

None

EMCB-RAI 6

In Section 5.1.3, [[ ]] page A30 (Reference 8), the following constraints are imposed on the water volume surrounding the bottom of the skirt:

a. [[ ]], although there are gaps between the steam separator tubes which allow the water to move radially.

b. [[ ]] Explain what is meant by "most nodes."

The above constraints increase the water loading on the immersed portion of the skirt and, therefore, they may impose unrealistic reduction of the skirt vibration response. Demonstrate the conservatism of these constraints with respect to the dynamic response and alternating stresses of the skirt.

GEH Response

[[

]]

a. [[

]]

b. [[

[1] [[ ]]

]]

Regarding the sentence in question, this sentence was poorly worded in NEDC-33824P, Appendix A. It is clarified to state:

"[[

]]"

[[

]]

Changes to NEDC-33824P Revision 0 – BFN Steam Dryer Analysis Report (SDAR):

NEDC-33824P, Appendix A, Section 5.1.3, fifth paragraph, last sentence states:

"[[

]]"

It will be revised to:

"[[

]]"

EMCB-RAI 7

[[

]] effectively includes damping in addition to the 1.0 percent structural damping in Section 4.2.1.4 of NEDC-33824P (Reference 6). Estimate the additional damping added to the dryer modes by [[

]]. Please also provide the properties (density, sound speed, damping, others) applied to the [[ ]]. Also, per Regulatory Guide 1.20, applying damping in addition to the usual allowable 1 percent requires justification. Provide full 120-second time histories of the Boiling-Water Reactor (BWR)/4 benchmark on-dryer SGs at EPU conditions in Matlab format, so that an independent assessment may be made to confirm the reasonableness of the added hydrodynamic damping caused by [[

]]

GEH Response

The steam dryer is in [[ ]]. The upper part of the dryer is [[

]] However, the lower part of the [[

]] become important in determining the overall [[

]] is to provide the Finite Element (FE) model with a somewhat [[

]] These results demonstrate that no additional damping is added to the metal structure [[ ]]

The following are the [[

]]

The requested time history data was provided to the NRC for an independent assessment in Reference 7-1.

Reference:

7-1. Letter from TVA to NRC, CNL-16-119, "Proposed Technical Specifications Change TS-505 - Request for License Amendments - Extended Power Uprate - Supplemental Information related to Replacement Steam Dryers," July 13, 2016.

Changes to NEDC-33824P Revision 0 – BFN Steam Dryer Analysis Report (SDAR):

None

EMCB-RAI 8

Figure 4.2-17 shows [[ ]] curves for [[ ]] structural analyses. [[ ]]. Since in this frequency range critical excitation frequencies associated with [[ ]] loading are present, it is nonconservative to have damping greater than 1 percent in these ranges.

a. Redefine the anchor points such that the damping is 1 percent or less over the entire frequency range of [[ ]]. Please provide the corresponding Minimum Alternating Stress Ratio (MASR) for the lead-in BFN RSD. Also explain how the [[ ]] is applied in the BWR/4 prototype dryer stress analyses.

b. Confirm that the Bias/Uncertainty (B/U) correction process accounts for excessive [[ ]]

   i. The licensee applies [[ ]] to their time domain analysis results per the procedures described in Section 4.2.5. Please confirm or clarify as appropriate the following staff's understanding of the approach.

      - The individual stress time histories [[ ]]
      - The amplitudes of important peaks in the resulting [[ ]] are combined with [[ ]] to compute weighted overall B/U corrections.
      - The [[ ]] are applied to the original peak values extracted from the time histories.

   ii. Given that the licensee uses a [[ ]] frequency resolution, quantitatively prove that bias corrections at the [[ ]] are conservative, considering that 1 percent damping implies a [[ ]] half-power bandwidth (which is much smaller than the [[ ]] resolution used). This proof may be based on demonstrating the procedure on simplified representative structural models.

   iii. Also, for the benchmark BWR/4 and BFN plants, the dead leg lengths are different [[ ]]. Provide:

      - The actual dead leg resonance frequencies at finer frequency resolution, including variability of these frequencies over time
      - The actual peak amplitudes at those frequencies and their variability over time

GEH Response

a. [[

]]

For the BWR/4 prototype [[ ]] analysis, a [[

]] RSD analysis. Thus any effect on vibration characteristics at [[

]] RSD analysis. However, the changes in the calculated [[

]]

In fact, results from the BWR/4 prototype benchmark analysis (with the same assumed damping as in the BFN RSD analysis) indicate that the [[

]]. Specifically, the benchmark results show that the strain predictions at [[

]] (see Table C5-1, Figures 4.5-1 and 4.5-2 in NEDC-33824P Appendix C). The benchmark comparisons show that the Rayleigh damping curves assumed in the BFN RSD analysis do not result in a non-conservative prediction of the stresses at 15 Hz.

The damping characteristics assumed in the BFN finite element analysis have no impact on the determination of the VPF contribution to the predicted RSD stresses. For the [[

]] is made through a [[

]]

(NEDC-33824P Section 4.1.5.4). This stress multiplier was determined from the individual strain measurements by [[

]]. The multipliers are based on the largest VPF signal measured in the prototype BWR/4 plant. Thus, the impact of the [[

]] curves are utilized.

[[ ]] Main Steam Line (MSL) dead leg frequency, the [[

]]. In addition, the [[
]] producing a conservative SRV load.

[[

]] biases and uncertainty values that are used to adjust the BFN final stress.

b. i. [[

]]

b. ii. As previously stated, the [[ ]] terms were applied to both the BWR/4 prototype [[ ]]. The impact of assuming a slightly higher damping value for the [[ ]] term ([[ ]]) would be conservative in regard to the bias term applied to the final calculation. Specifically, a higher damping value would result in under-predicting the strain for [[

]]

Consequently, the impact of using a slightly [[ ]] on the benchmark would result in a [[

]] in order to quantitatively compare the effect of the assumed damping. From NEDC-33824P Appendix C, Table C5-1, the lower dryer end-to-end bias value is [[ ]]. The change in the assumed [[

]]

[[

]]

Figure 8-1a. [[

]]

Figure 8-1b shows the predicted strain time history for [[

]] On average (for the [[ ]]), the actual [[ ]] (stress equivalent) in the time signal increased by [[ ]]

It should be noted that the damping curve between the two pinning frequencies is below 1%. [[

]]

As with the [[ ]], the change in the predicted strain at different frequencies for the BWR/4 prototype benchmark [[

]]

[[

]]

Figures 8-1b and 8-1c (zoom). [[

]]

In addition, Figure 8-2 is included to show another [[ ]] and how the [[

]]

[[

]]

Figure 8-2. [[

]]

The question relative to what the impact might be of using a [[

]]

Secondly, the [[
]] The load signal has energy in the 15 Hz band. [[

]]

b. iii. In order to compare the resonances in the [[
]] to estimate any differences in signal. Comparison plots were made for different [[
]]. In addition, plots were made to characterize the [[
]]. In particular, the MSL pressure data was analyzed using the PWELCH function using 85 time segments taken over ~120 seconds of data.

[[
]] Plots were developed for the upper strain gauge locations for these MSLs. Specifically, the following plots were developed for each:

1. Dot plot of amplitude distribution at each frequency bin (14.0 Hz to 16.0 Hz)
2. Plot pair for sample number versus peak frequency and sample number versus amplitude for peak frequency (from 14.5 Hz to 16.0 Hz) each. These plots provide an approximation of the peak amplitude and peak frequency variation over time.

As can be seen in Figures 8-3 through 8-10, both the [[
]] resonant frequency.

[[
]]

The time segment history plots provided below illustrate the variability in the amplitude and frequency over time [[ ]].

[[

]]

Figure 8-3. [[

]]

[[

]]

Figure 8-4. [[ ]] **Frequency/Amplitude Versus Time Segment**

[[

]]

Figure 8-5. [[

]]

[[

]]

Figure 8-6. [[ ]] **Frequency/Amplitude Versus Time Segment**

[[

]]

Figure 8-7. [[

]]

[[

]]

Figure 8-8. [[ ]] **Frequency/Amplitude Versus Time Segment**

[[

]]

Figure 8-9. [[

]]

[[

]]

Figure 8-10. [[ ]] **Frequency/Amplitude Versus Time Segment**

Changes to NEDC-33824P Revision 0 – BFN Steam Dryer Analysis Report (SDAR):

None

EMCB-RAI 12

In Section 4.2.1.7 of NEDC-33824P (page 4-119) it is stated that, [[
]] Provide the value for the coefficient of friction and the magnitude of the friction force during heat-up and cooldown. Justify [[ ]] in the dryer stress analysis.

GEH Response

A specific value for the friction force due to heat-up and cooldown is difficult to define due to variations in surface roughness, cleanliness, and lubrication on the steam dryer support bracket. Machinery's Handbook 29th edition (Reference 12-1) lists the coefficient of static friction of steel on steel as varying between the clean unlubricated surface value of 0.8 to a lubricated surface value of 0.16. In addition, [[

]] due to differential thermal expansion of the dryer and the Reactor Pressure Vessel (RPV).

The mount point boundary condition could be modeled several ways in the Flow-Induced Vibration (FIV) analysis. The options to model the mount point boundary condition are as follows; [[

]]. Regarding Option 1, [[

]] The associated stiffness with this friction would [[
]]. Therefore, to constrain the radial direction [[

]]. For these reasons, [[

]]

GE Hitachi Nuclear Energy (GEH) recognizes the [[ ]] the actual structure during operation; however, analysis accounts for this discrepancy in two ways.

As discussed in Section 6.1.1 of NEDC-33824P of Appendix A (page A-50), [[

]] will therefore account for some variation in [[ ]]. Likewise, the [[ ]] at the mount point, [[ ]] will therefore cover differences in the response due to the [[ ]].

Reference:

12-1 Machinery's Handbook, 29th Edition, Industrial Press, Inc., January 16, 2012.

Changes to NEDC-33824P Revision 0 – BFN Steam Dryer Analysis Report (SDAR):

None

EMCB-RAI 20

The [[
]]. As illustrated in NEDC-33824P on page 4-54 (Reference 6), the dryer load amplitude is very sensitive to changes in the frequency or phase of the SRV acoustic sources. The licensee is requested to explain how the [[
]] during the dryer stress computation.

GEH Response

Phasing between the Main Steam Line (MSL) is relative, not absolute. To account for structural uncertainty, [[
]] will not change the relative phasing of the MSL signal, just the absolute phase.

Changes to NEDC-33824P Revision 0 – BFN Steam Dryer Analysis Report (SDAR):

None

EMCB-RAI 23

In Section 4.1.4.2 of NEDC-33824P (page 4-42 of Reference 6), it is noted that previous testing and analysis has indicated that High Pressure Coolant Injection, Reactor Core Isolation Cooling, and vent lines are [[ ]]. Explain, if the first valve (from the MSL) on any of the three lines is closed (an off-normal event), why that line [[ ]]. Provide a history of such off-normal events at BFN plants, and the impact of those events on steam dryer analysis.

GEH Response

These piping runs will not cause any appreciable fatigue accumulation on the steam dryer as the result of acoustic resonances due to a closed valve in the piping lines during Extended Power Uprate (EPU) conditions. The argument for each of these three piping runs is given below in bullet items 1 through 3:

1. The High Pressure Coolant Injection (HPCI) is on the B-Line dead leg and thus has no steady-state steam flow past the branch line opening regardless of the HPCI isolation valve position. Because there is no driving force for creating a resonance, there is no concern for a related resonance generated loading of the steam dryer as a result of the HPCI piping line.

   The HPCI line is only isolated by valve for quarterly testing or maintenance (limited by the 14 day Limiting Conditions for Operation (LCO)).

   Hence, there is no concern with any additional fatigue loading being introduced as a result of resonances in the HPCI piping system.

2. The reactor head vent line connects the vessel head region to Main Steam Line (MSL) C just downstream of the first elbow from the vessel. This line is open at all times during operation. The only valve on this line is one manual valve located in the dry well and thus it cannot be closed during operation. The purpose of this vent line is to draw non-condensible gases from the vessel head region and exhaust them into the steam line and on to the condenser. The pressure difference between the vessel head region and the steam line creates a continuous flow through the vent line. The flow exiting the vent line into the steam line will prevent a shear layer vortex from forming across the opening. Therefore, it is not possible to generate an acoustic resonance in the vent line.

   Hence, there is no concern with any additional fatigue loading being introduced as a result of resonances in the head vent piping system.

3. The Reactor Core Isolation Cooling (RCIC) is on the C-Line in the MSL flow path between the vessel and the turbine. Thus, there is steam flow across the branch opening during operation. However, the RCIC steam line is 3” Schedule 160 piping. It is not considered likely that a side branch with a d=2.624” Inside Diameter (ID) on a

D=23.358" diameter pipe (26" Schedule 80) with d/D = 0.112 will generate an acoustic resonance that can cause substantial pressure loading on the dryer. The isolation valve for the RCIC system is greater than 20 feet from the intersection. There are two reasons that if there is an acoustic resonance, it will be negligible:

- The small diameter of the branch line means that the potential resonance frequency that can be supported during full power operation by the shear layer vortex will be high –approximately [[ ]].
- With a branch line greater than 20 feet long, the acoustic resonance is going to be a higher order harmonic of the fundamental mode standing wave frequency (more than [[ ]] quarter wavelengths at [[ ]]). Thus, the excitation of the RCIC steam line would not create a significant acoustic load on the dryer.

The RCIC is only isolated by valve for quarterly testing or maintenance (limited by the 14 day LCO).

Hence, it is concluded that any loads that might be generated due to a resonance in the RCIC line would be of very low amplitude and would not produce any appreciable number of fatigue cycles over the design life of the dryer.

Changes to NEDC-33824P Revision 0 – BFN Steam Dryer Analysis Report (SDAR):

None

EMCB-RAI 25

In Section 4.1.7.4 of NEDC-33824P (pages 4-89 to 4-101 of Reference 6), several features of the dryer acoustic loading of BFN are compared with those of other plants, including the [[ ]]. In these comparisons, the acoustic pressure characteristics are [[ ]]. This type of comparison between averages does not reflect the degree of local differences and may result in underestimating the maximum dryer stress. Since the [[ ]] is considered to be the prototype for the BFN plant, it would be appropriate to first validate this assumption by comparing the individual acoustic sources at the MSL nozzles of both plants. This comparison is needed to substantiate the [[ ]]. Therefore, the licensee is requested to compare the acoustic sources at the MSL inlets for BFN and the prototype plant at CLTP conditions. These sources can be estimated by means of MSL data based plant based load evaluation [[ ]] methodology. Please provide overlaid Power Spectral Density (PSDs) of the sources for each MSL separately.

GEH Response

The intent of the comparisons [[

]] The outcome from these comparisons was [[

]]

NEDC-33824P Section 4.1.7 presented different ways to compare the acoustic characteristics of the two plants [[

]]

It should be noted that the key [[

]]

NEDC-33824P presented summaries of these comparisons [[

]]

In fact, a review of [[

]] is a good

representation of the similarity of the acoustic pressure loads between the [[
]].

Note that the FIV stress analysis is performed by mapping the steam dryer acoustic nodal pressure (a total of [[ ]] nodes) onto the structural Finite Element (FE) model. The FIV analysis is performed with a very fine degree of localization, [[
]]

The main concern raised by Request for Additional Information (RAI)-25 [[

]]

The following are additional discussions and comparison plots [[

]]

Also, this RAI response includes a discussion of the comparison between [[
]]

[[ ]]

NEDC-33824P presented, in Figure 4.1-48, the BFN [[
]].

Figure 4.1-48 shows [[ ]]. However, NEDC-33824P also presented, in Figures 4.1-49 and 4.1-50, the BFN vs. [[ ]] Acoustic FRFs Pressure Distribution (3D plots) at several peak frequencies [[
]]. A large similarity is observed in these figures, particularly the large similarity over every local area of the BFN and [[ ]] steam dryers.

More discussion is presented in NEDC-33824P Section 4.1.7.4.a.

[[ ]]

NEDC-33824P Figure 4.1-52 presented a comparison of BFN Unit 1 [[

]].

It was preferred to present the MSL pressure PSD as [[

]]

The advantage of the measured MSL comparison [[
]]

The intent of the MSL pressure comparisons [[

]]

It was indicated that it would be appropriate to [[

]]

Independently, it does not matter so much [[

]]. See the next sub-section (On-Dryer Pressure Loads) for the on-dryer pressure loads comparison and the noted degree of local similarities between the two plants.

In addition to the [[ ]], the main body of NEDC-33824P and NEDC-33824P Appendix D did include several MSL pressure comparisons per [[

]].

NEDC-33824P (Main Body):

[[

]]

NEDC-33824P Appendix D Figures 4-1 to 4-13:

[[

]]

[[ ]]

The on-dryer pressure loads comparisons are the more appropriate comparisons [[
]]

The FIV analysis is performed by mapping the steam dryer acoustic nodal pressure (a total of [[ ]] nodes) on the structural FE model. The stress analysis is directly related to the on-dryer pressure loads, [[

]].

NEDC-33824P Figure 4.1-53 presented a summary comparison of BFN [[

]].

To reflect the degree of local differences, additional comparison plots are included in the present RAI response.

[[

]]

Appendices A-1 to A-4 present additional comparison [[

]]

MSL Dead-Legs [[ ]]:

MSL Measurement:

From the MSL pressure measurements (NEDC-33824P Figure 4.1-51 and NEDC-33824P Appendix D Figures 4-1 to 4-13), [[
]].

Calculated [[ ]] Dryer Pressure Loads:

From the calculated [[ ]] pressure loads (NEDC-33824P Figure 4.1-53), and present RAI response (Appendices A-1 to A-4), [[
]]

[[

]]

Changes to NEDC-33824P Revision 0 – BFN Steam Dryer Analysis Report (SDAR):

[[

]]

[[

]]

[[

]]

Appendix A1

[[

]]

Figure A1-1: [[ ]]

Figure A1-2: [[ ]]

Figure A1-3: [[ ]]

Figure A1-4: [[ ]]

Figure A1-5: [[ ]]

Figure A1-6: [[ ]]

[[

]]

Figure A1-1: [[

]]

[[

]]

Figure A1-2: [[

]]

[[

]]

Figure A1-3: [[

]]

[[

]]

Figure A1-4: [[

]]

[[

]]

Figure A1-5: [[

]]

[[

]]

Figure A1-6: [[

]]

Appendix A2

[[

]]

Figure A2-1: [[ ]]

Figure A2-2: [[ ]]

Figure A2-3: [[ ]]

Figure A2-4: [[ ]]

Figure A2-5: [[ ]]

Figure A2-6: [[ ]]

[[

]]

Figure A2-1: [[

]]

[[

]]

Figure A2-2: [[

]]

[[

]]

Figure A2-3: [[

]]

[[

]]

Figure A2-4: [[

]]

[[

]]

Figure A2-5: [[

]]

[[

]]

Figure A2-6: [[

]]

Appendix A3

[[

]]

Figure A3-1: [[ ]]

Figure A3-2: [[ ]]

Figure A3-3: [[ ]]

Figure A3-4: [[ ]]

Figure A3-5: [[ ]]

Figure A3-6: [[ ]]

[[

]]

Figure A3-1: [[

]]

[[

]]

Figure A3-2: [[

]]

[[

]]

Figure A3-3: [[

]]

[[

]]

Figure A3-4: [[

]]

[[

]]

Figure A3-5: [[

]]

[[

]]

Figure A3-6: [[

]]

Appendix A4

[[

]]

Figure A4-1: [[ ]]

Figure A4-2: [[ ]]

Figure A4-3: [[ ]]

Figure A4-4: [[ ]]

Figure A4-5: [[ ]]

Figure A4-6: [[ ]]

[[

]]

Figure A4-1: [[

]]

[[

]]

Figure A4-2: [[

]]

[[

]]

Figure A4-3: [[

]]

[[

]]

Figure A4-4: [[

]]

[[

]]

Figure A4-5: [[

]]

[[

]]

Figure A4-6: [[

]]

Appendix B1

[[ ]]

[[

]]

Figure B1.1: [[ ]]

[[

]]

Figure B1.2: [[

]]

[[

]]

Figure B1.3: [[

]]

[[

]]

Figure B1.4: [[

]]

[[

]]

Figure B1.5: [[

]]

[[

]]

Figure B1.6: [[

]]

[[

]]

Figure B1.7: [[

]]

EMCB-RAI 28

In Appendix E (Reference 10) of NEDC-33824P, Table 4.4-1 on Page E22 shows locations of the SGs that will be installed on the MSLs. The locations of the [[
]]. However, the locations of the lower gages are different. Please explain the differences between the arrangements of the MSLs in the three units that preclude installing the lower gages at similar locations in the three units.

GEH Response

The Browns Ferry Nuclear Plant (BFN) Extended Power Uprate (EPU) program has taken place over many years. The original design intent was to site all three units strain gauge locations with a similar spacing arrangement. However, due to a mix of practical challenges encountered during the installation, the preliminary or original locations were moved to avoid problems associated with the installation work site.

For BFN Unit 1, [[
]]

For BFN Unit 2, [[
]] This alternate location was developed during initial strain gauge installation for Unit 2 in 2006.

For BFN Unit 3, [[
]]

Given that the locations for all three units are not exactly the same, a review of the spacing was performed during the data screening and acoustic load generation activities. [[

]]

[[

]]

Changes to NEDC-33824P Revision 0 – BFN Steam Dryer Analysis Report (SDAR):

None

EMCB-RAI 33

GEH has benchmarked the [[

]]. Provide the following additional information regarding the benchmarking.

Provide PSD plots for both [[ ]] based benchmarking that show that all peak strains at all measured SG locations are bounded by the upper envelope of the [[

]]. If any peak strains are not bounded, provide an assessment of the nonconservatism(s) on dryer fatigue life.

GEH Response

[[

]] benchmark evaluation was performed utilizing loads developed from [[

]]

The individual PSD plots are informative for qualitatively looking at resonances. [[

]] Figures 33-19 through 33-27 compare the predicted strains to the measured strains for the [[

]] The cumulative strain plots are shown in Figures 33-28 through 33-36. Additionally, it is important to consider that [[

]]

Other peaks are observed at higher frequencies [[

]]

A few of the strain gauges show a measured data peak at approximately [[

]] is described in NEDC-33824P Section 4.1.4.

[[

]] will ensure that the margins from on-dryer measurements remain conservative.

[[

]]

Figure 33-1: Strain Gauge 1 [[ ]] **Evaluation**

[[

]]

Figure 33-2: Strain Gauge 2 [[ ]] **Evaluation**

[[

]]

Figure 33-3: Strain Gauge 3 [[ ]] **Evaluation**

[[

]]

Figure 33-4: Strain Gauge 4 [[ ]] **Evaluation**

[[

]]

Figure 33-5: Strain Gauge 5 [[ ]] **Evaluation**

[[

]]

Figure 33-6: Strain Gauge 6 [[ ]] **Evaluation**

[[

]]

Figure 33-7: Strain Gauge 7 [[ ]] **Evaluation**

[[

]]

Figure 33-8: Strain Gauge 8 [[ ]] **Evaluation**

[[

]]

Figure 33-9: Strain Gauge 9 [[ ]] **Evaluation**

[[

]]

Figure 33-10: Strain Gauge 1 [[ ]] **Evaluation**

[[

]]

Figure 33-11: Strain Gauge 2 [[ ]] **Evaluation**

[[

]]

Figure 33-12: Strain Gauge 3 [[ ]] **Evaluation**

[[

]]

Figure 33-13: Strain Gauge 4 [[ ]] **Evaluation**

[[

]]

Figure 33-14: Strain Gauge 5 [[ ]] **Evaluation**

[[

]]

Figure 33-15: Strain Gauge 6 [[ ]] **Evaluation**

[[

]]

Figure 33-1: Strain Gauge 7 [[ ]] **Evaluation**

[[

]]

Figure 33-17: Strain Gauge 8 [[ ]] **Evaluation**

[[

]]

Figure 33-18: Strain Gauge 9 [[ ]] **Evaluation**

[[

]]

Figure 33-19: Strain Gauge 1 [[ ]] **Evaluation PSD Band Summation**

[[

]]

Figure 33-20: Strain Gauge 2 [[ ]] **Evaluation PSD Band Summation**

[[

]]

Figure 33-21: Strain Gauge 3 [[ ]] **Evaluation PSD Band Summation**

[[

]]

Figure 33-22: Strain Gauge 4 [[ ]] **Evaluation PSD Band Summation**

[[

]]

Figure 33-23: Strain Gauge 5 [[ ]] **Evaluation PSD Band Summation**

[[

]]

Figure 33-24: Strain Gauge 6 [[ ]] **Evaluation PSD Band Summation**

[[

]]

Figure 33-25: Strain Gauge 7 [[ ]] **Evaluation PSD Band Summation**

[[

]]

Figure 33-26: Strain Gauge 8 [[ ]] **Evaluation PSD Band Summation**

[[

]]

Figure 33-27: Strain Gauge 9 [[ ]] **Evaluation PSD Band Summation**

[[

]]

Figure 33-28: Strain Gauge 1 [[ ]] **Evaluation Cumulative Strain**

[[

]]

Figure 33-29: Strain Gauge 2 [[ ]] **Evaluation Cumulative Strain**

[[

]]

Figure 33-30: Strain Gauge 3 [[ ]] **Evaluation Cumulative Strain**

[[

]]

Figure 33-31: Strain Gauge 4 [[ ]] **Evaluation Cumulative Strain**

[[

]]

Figure 33-32: Strain Gauge 5 [[ ]] **Evaluation Cumulative Strain**

[[

]]

Figure 33-33: Strain Gauge 6 [[ ]] **Evaluation Cumulative Strain**

[[

]]

Figure 33-34: Strain Gauge 7 [[ ]] **Evaluation Cumulative Strain**

[[

]]

Figure 33-35: Strain Gauge 8 [[ ]] Evaluation Cumulative Strain

[[

]]

Figure 33-36: Strain Gauge 9 [[ ]] Evaluation Cumulative Strain

Changes to NEDC-33824P Revision 0 – BFN Steam Dryer Analysis Report (SDAR):

None

EMCB-RAI 35

Link the five most stressed upper dryer locations and five most stressed lower dryer locations to specific on-dryer SGs. Show pictorially the gage and peak stress locations at the frequencies most responsible for peak stresses.

GEH Response

From NEDC-33824P Table 4.4-1, Table 35-1 lists the six lowest Alternating Stress Ratio (ASR) components in the upper dryer region and the five lowest ASR components in the lower dryer region. Table 35-1 also provides a correlation for the sensors that best monitor the spectral behavior at the respective stress location. The sensor locations are chosen by a [[

]] In addition to the table, Figures 35-1 through 35-3 pictorially show the [[ ]] that are listed in the table (the figures use the "Location" column for the callout of a particular stress location).

Table 35-1. Sensor to Component Mapping

Location	Upper Region Components	ASR	Sensors	
[[				
				]]
Location	**Lower Region Components**	**ASR**	**Sensors**	
[[				
				]]

[[

]] Figures 35-4 through 35-14 provide Power Spectral Density (PSD) plots for the respective components in Table 35-1. These PSD curves are generated from the [[

]]

[[

]]

Figure 35-1

[[

]]

Figure 35-2

[[

]]

Figure 35-3

[[

]]

Figure 35-4

[[

]]

Figure 35-5

[[

]]

Figure 35-6

[[

]]

Figure 35-7

[[

]]

Figure 35-8

[[

]]

Figure 35-9

[[

]]

Figure 35-10

[[

]]

Figure 35-11

[[

]]

Figure 35-12

[[

]]

Figure 35-13

[[

]]

Figure 35-14

Changes to NEDC-33824P Revision 0 – BFN Steam Dryer Analysis Report (SDAR):

None

EMCB-RAI 38

The limits in Table 5.3.1 (time) and Appendix E-1 (frequency) appear to be nonconservative compared to strains observed in other instrumented dryers.

a. Compare the simulated on-dryer strains for the BFN dryer to those measured on the benchmark BWR/4 dryer.

b. Provide cumulative strain plots for sensors [[ ]] to complement the computing root mean square (RMS) values provided in Table 5.3-1.

c. SGs 6 and 9 have very high potential strains – up to [[ ]]. SGs have a finite life, particularly at high amplitude. Provide information on which frequency(s) contribute most strongly to the strain at these gage locations Describe the survivability (expected life or number of cycles) of the dryer SGs at these potential strain amplitudes.

d. Provide alternative procedures for RMS limits and frequency-dependent limit curves for on-dryer SGs based on new data acquired on the lead BFN dryer just prior to power ascension to CLTP. Note that since these methods would be based on data measured on the BFN dryer, [[ ]]. The current simulations of on-dryer strains may be used to demonstrate the procedure, but not used as actual limits during power ascension.

GEH Response

a. For comparison, the analysis scenario of the Browns Ferry Nuclear Plant (BFN) dryer Finite Element Analysis (FEA) model applied with the [[

]] was run, which is referred to as 'BFN, CR Load' later in the presented plots. In this particular analysis, [[

]]

The rationale for using the analysis [[

]]

[[

]]

Figure 38a-1. [[ ]]

[[

]]

Figure 38a-1. [[ ]]

[[

]]

Figure 38a-2. [[

]]

[[

]]

Figure 38a-3. [[

]]

[[

]]

Figure 38a-4. [[

]]

[[

]]

Figure 38a-5. [[

]]

[[

]]

Figure 38a-6. [[

]]

[[

]]

Figure 38a-7. [[

]]

[[

]]

Figure 38a-8. [[

]]

[[

]]

Figure 38a-9. [[

]]

[[

]]

Figure 38a-10. [[

]]

[[

]]

Figure 38a-11. [[

]]

[[

]]

Figure 38a-12. [[

]]

[[

]]

Figure 38a-13. [[

]]

[[

]]

Figure 38a-14. [[

]]

[[

]]

Figure 38a-15. [[

]]

[[

]]

Figure 38a-16. [[

]]

[[

]]

Figure 38a-17. [[

]]

[[

]]

Figure 38a-18. [[

]]

[[

]]

Figure 38a-19. [[

]]

b. To complement [[

]]

It is necessary to stress that [[

]]

As described in Section 5.4 of NEDC-33824P Appendix E, [[

]]

[[

]]

Figure 38b-1. [[

]]

[[

]]

Figure 38b-2. [[

]]

[[

]]

Figure 38b-3. [[

]]

[[

]]

Figure 38b-4. [[

]]

[[

]]

Figure 38b-5. [[

]]

[[

]]

Figure 38b-6. [[

]]

[[

]]

Figure 38b-7. [[

]]

[[

]]

Figure 38b-8. [[

]]

[[

]]

Figure 38b-9. [[

]]

[[

]]

Figure 38b-10. [[

]]

[[

]]

Figure 38b-11. [[

]]

[[

]]

Figure 38b-12. [[

]]

Table 38b-1. [[

]]

[[							
							]]

c. [[

]]

Table 38c-1: [[

]]

[[	
	]]

The use of the Ni-Cr-Fe fatigue Curve C (Figure 38c-1) from the American Society of Mechanical Engineers (ASME) Section III (Division 1, Appendix I, 1995) for the fatigue evaluation on the strain gage product (with the wire made of Ni-CrV) is considered conservative.

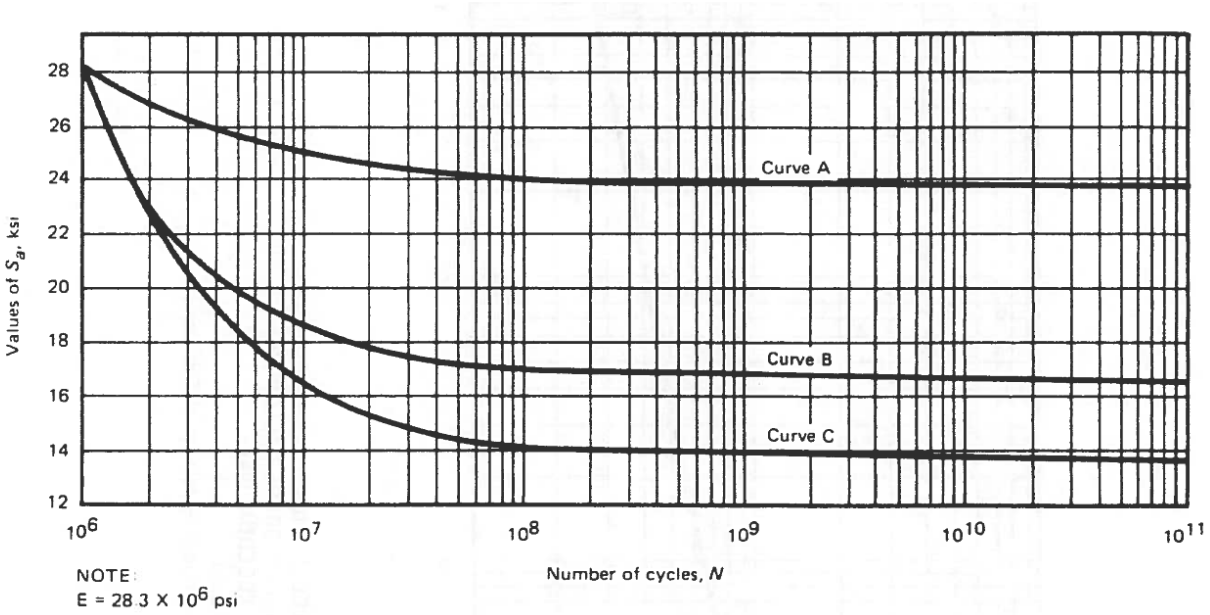

Figure 38c-1 (Figure I-9.2.2) Design Feature Curves for Austenitic Steels, Nickel-Chromium-Iron Alloy, Nickel-Iron-Chromium Alloy, and Nickel-Copper Alloy for Sa ≤ 28.2 ksi, for Temperatures Not Exceeding 800°F (For Sa>28.2 ksi, use Figure I-9.2.1)

The strain gage product specification and some supplementary test data from the manufacturer can be used to address the survivability of the strain gages. The strain gages of Model 'KHC-10-120' supplied by Kyowa Electronic Instruments Co., Ltd (Kyowa) has been and continue to be used in the BWR/4 and BWR/6 dryer EPU instrumentation process. In the product specification, the fatigue life at room temperature is identified as 4×10^5 (±1000μm/m), (i.e., 4×10^5 cycles with strain level ±1000 με (micro-strain)). The extra supplementary test data were provided by Kyowa and summarized in Table 38c-2. The test results were available in a paper (Reference 38-1) published in conjunction with the Japan Atomic Energy Research Institute (JAERI) in November 1983.

Table 38c-2: Comparison of KYOWA Fatigue Test Data with [[ ]]

	Operation Temperature	**Strain Level (με)**	**Fatigue Life (cycles)**	**Strain Gage Integrity Hold/Not?**
KHC Product Specification	75.2°F (24° C)	±1000	4×10^5	No information provided
KHC Test 1	932°F (500° C)	±300	$1x10^7$	Strain gage is not reported broken
KHC Test 2		**±1000**	**$2x10^6$**	**Strain gage is reported broken**
KHC Test 3		±500	$5x10^6$	Strain gage is not reported broken

[[

]] the time duration required for the power ascension test to complete, which is [[ ]].

d. The procedure for the Root Mean Square (RMS) limits and frequency-dependent limit curves for on-dryer Strain Gages (SGs) based on new data acquired on the lead BFN dryer is [[ ]]

Appendix E presented the power ascension test plan and limit curves (on-dryer and Main Steam Line (MSL) based) for the Browns Ferry Nuclear Plant (BFN) replacement steam dryers. Section 5.0 of Appendix E discussed the [[ ]] limit curves for on-dryer strain gages based on the Flow-Induced Vibration (FIV) analysis results developed from [[

]]

Lead unit power ascension process was presented in Appendix E, Figure 3.2-1. [[

]]

It is noted that for BFN dryer limit curve updates with the BFN on-dryer measurements, [[

]]

The methodology for maximum stress calculation and acceptance limit updates with on-dryer strain measurement is consistent [[

]]

[[

]]

Figure 38d-1. [[

]]

As presented in the [[ ]] Figure 3.2-1 [[

]]

Measured Data:

[[ ]]

Predicted Data:

[[

]]

Reference

38-1. Evaluation Test of Stability for High Temperature Strain Gages (in Japanese), 共和技報, No. 309, November 1983.

Changes to NEDC-33824P Revision 0 – BFN Steam Dryer Analysis Report (SDAR):

Appendix E: Power Ascension Test Plan Limit Curves (On-Dryer & MSL Based)

[[

]]

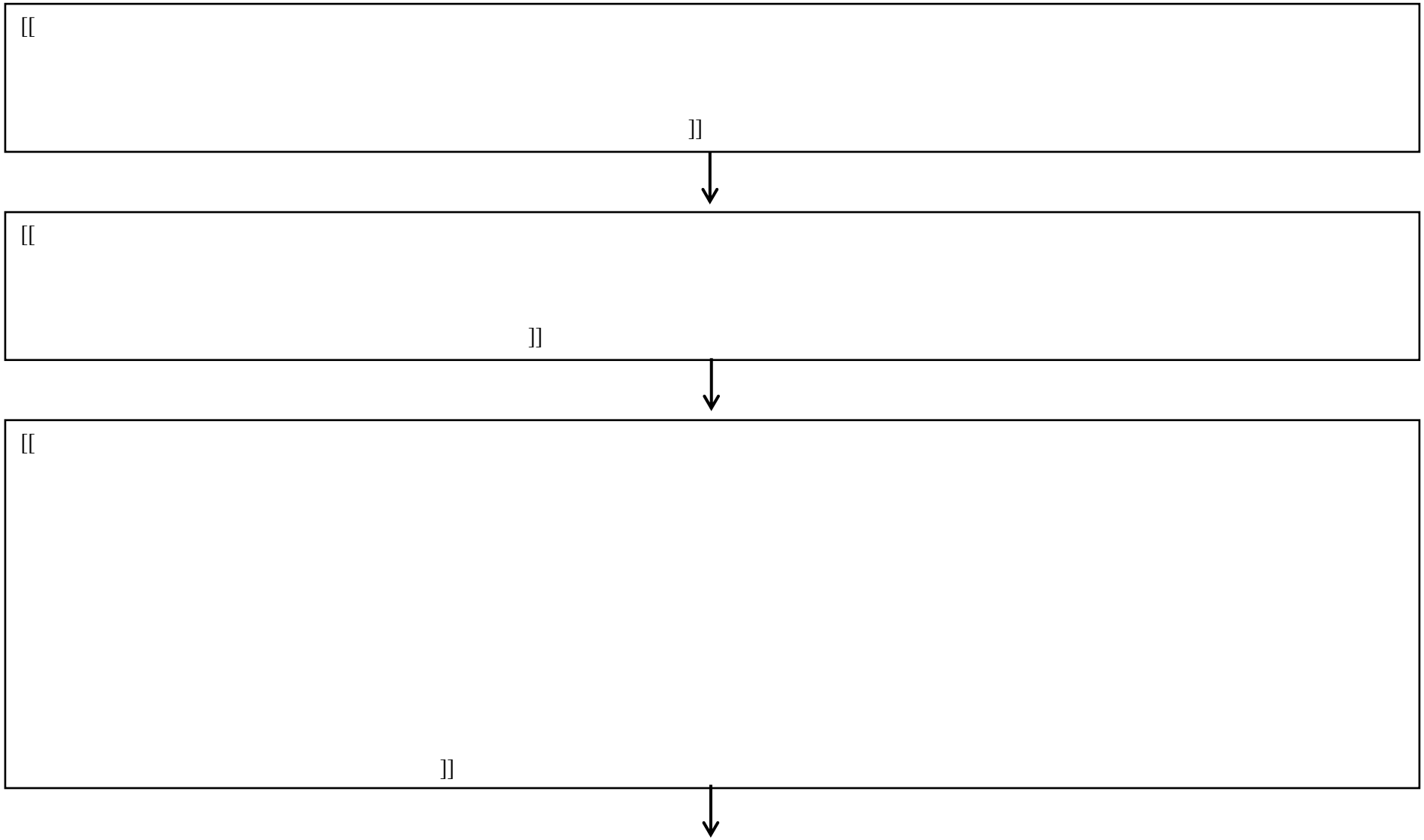

(continued on next page)

Figure 3.2-1: Browns Ferry [[ ]]

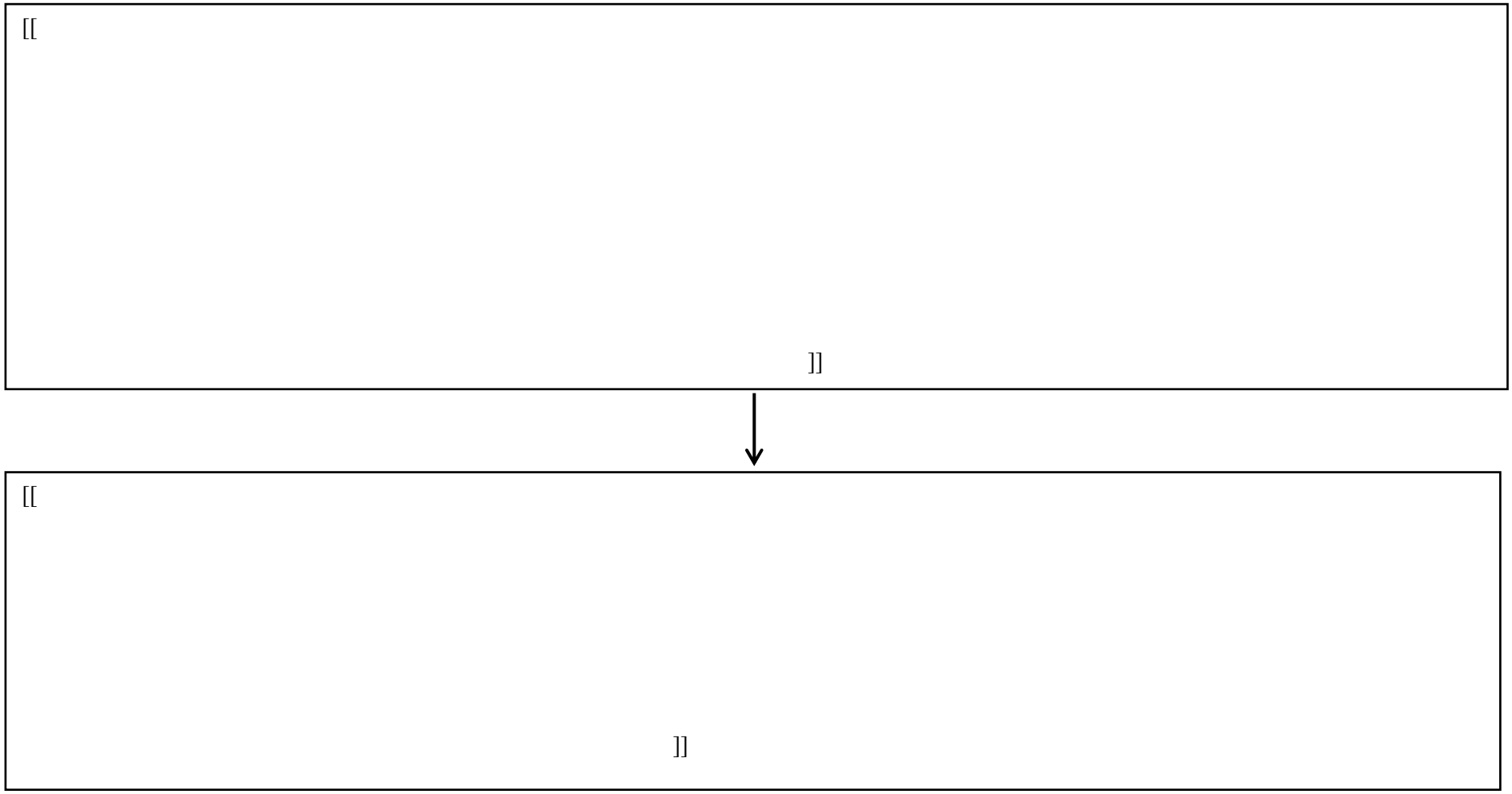

Figure 3.2-1: Browns Ferry [[ ]] **(continued)**

EMCB-RAI 39

GEH computes [[

]]. The final alternating stress ratios (ASRs) at EPU shown in Table 4.4-1 on pages 4-152 and 4-153 (Reference 6) are above 2.0, and additional details of the five most highly stressed dryer regions are provided in Section 6 of Appendix D (Reference 10) of Attachment 40 (Ref. 6). However, not enough peak stress locations were addressed in the plots provided. Provide the following additional information.

a. Table 8.1-4 of Appendix-A (p. A-88 of Reference 8) states that a [[

]]. Provide the numerical value of the [[ ]] used in the static analysis. Also, provide a justification for the magnitude of the [[ ]] value.

b. The instrument mast on BFN unit 3 RSD used for on-dryer instrumentation may influence the dryer stresses in the vicinity of the mast. Please clarify the following:

   i. Are the ASRs shown in Table 4.4-1 (pages 4-152 and 4-153 of Reference 6) based on a structural finite element model of the RSD with the instrumentation mast, without the instrumentation mast or an envelope of with and without the mast?

   ii. If the ASRs in Table 4.4-1 are based on a dryer model without the mast, provide ASRs for a model that includes the mast.

c. Based on Section 5.1 (page 5-1), and Section 4.1 (p. A-16) of Appendix-A (Reference 8) it appears that the ASRs shown in Table 4.4-1 are [[

]]. This issue is being discussed in the ASME Code committees, and has not been resolved. Therefore, provide adjusted Table 4.4-1 ASRs applying the [[

]]

d. Provide spectra and stress accumulation plots for the five most highly stressed upper dryer and for the five most highly stressed lower dryer locations. Highlight the relative contributions to total stress of the [[ ]], the SRV resonance peak(s), and the VPF peak.

GEH Response

a. The acoustic load on the face of the steam dryer hood during a Main Steam Line Break (MSLB) event consists of [[

]]

Figure 39-1 shows an example of the typical [[ ]] time histories for several points on the dryer hood. The [[ ]] at each location on the dryer hood can be obtained from the corresponding [[ ]] time history as shown in Figure 39-1. The acoustic loads applied on the steam dryer outer hood for the MSLB are obtained by applying the [[ ]]. To account for the dynamic effect from the MSLB transient event [[ ]]. This factor is defined [[ ]]. Because deflection, spring forces, and stresses in the linear elastic structure analysis are all proportional, the [[ ]]. In Reference 39-1 the responses for one-degree elastic systems (un-damped) subjected to symmetrical triangular load pulse are calculated. Figure 39-2 (Figure 2.6(c) in Reference 39-1) shows the typical responses for this type of forcing function which start at zero and reach a maximum F1 at one-half the total force duration t_d, with T as the natural period of the system. The maximum response as a function of t_d/T is given by Figure 39-3 (Figure 2.8(a) in Reference 39-1). [[ ]] As shown in Figure 39-1, the time histories of MSLB acoustic loads [[

]]

[[

]]

Figure 39-1. Typical Local Normalized Pressure vs Time and Peak Normalized Pressure Loads on the Hood

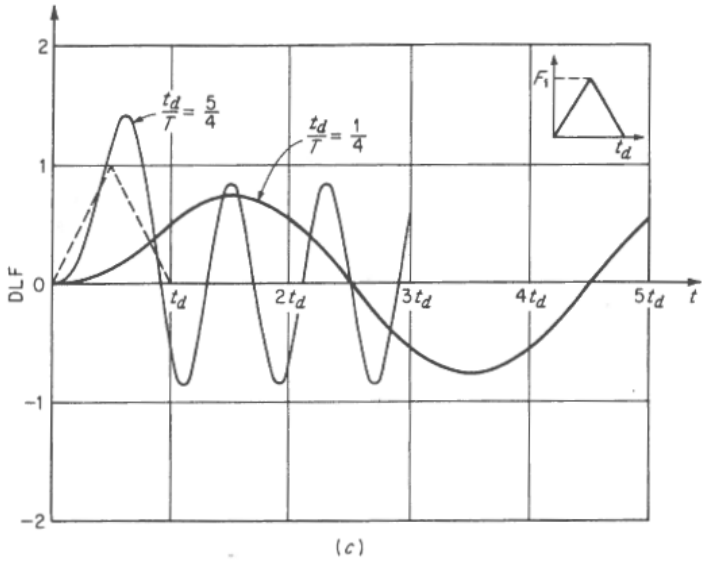

Figure 39-2. Typical Responses of One-Degree Elastic Systems (Un-damped) Subjected to Symmetrical Triangular Load Pulse (T is the natural period of the system)

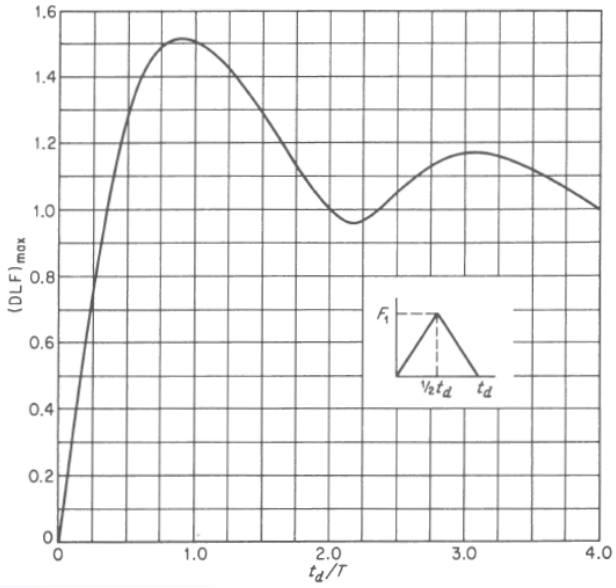

Figure 39-3. Maximum Response of One-Degree Elastic Systems (Un-damped) Subjected to Symmetrical Triangular Load Pulse (T is the natural period of the system)

b. [[

]]

Although the dryer Finite Element Model (FEM) used to generate Flow-Induced Vibration (FIV) ASR values [[

]]

To evaluate the global impact of the instrumentation mast [[
]] the RSD with and without the instrumentation mast was performed up to frequency of [[ ]], which covered the [[
]]. Resulting [[
]] by inclusion of the instrumentation mast in the model. Additionally, a selected [[ ]] was performed to evaluate the [[

]]

Figure 39-4 shows the structural finite element model of the RSD with the instrumentation mast model, [[ ]]. Table 39-1 is the [[
]] are shown in Figures 39-5, 39-6, and 39-7, which are mainly the [[ ]]. Global steam dryer [[
]]. From Figures 39-8 and 39-9, the [[
]].

[[

]]

Figure 39-4. [[ ]]

Table 39-1: [[ ]]

[[

]]

[[

]]

Figure 39-5. [[ ]]

[[

]]

Figure 39-6. [[ ]]

[[

]]

Figure 39-7. [[ ]]

[[

]]

Figure 39-8. Steam Dryer Modes at [[ ]]

[[

]]

Figure 39-9. Steam Dryer Modes at [[ ]]

To evaluate the [[ ]], the FIV stress analysis is performed to the [[

]]. The stress intensity contour plot of the component of [[ ]] is shown in Figure 39-10. The maximum stress intensity is at [[

]] is shown in Figure 39-11. The instrumentation mast is [[

]] in Figure 39-11. [[

]] When excluding the stress at these [[ ]] as shown in the close look of the [[ ]] at the bottom left of Figure 39-12, which is [[

]] as shown in Figure 39-12. [[

]] as shown in Figure 39-13, [[

]]

[[

]]

Figure 39-10. [[

]]

[[

]]

Figure 39-11. [[ ]]

[[

]]

Figure 39-12. [[

]]

[[

]]

Figure 39-13. [[

]]

In addition, all the mast structure components have been analyzed for [[

]]

c. ASRs shown in Table 4.4-1 are [[ ]]. For components with stresses calculated directly from the FEM, [[

]] from NEDC-33824P shows that a few limited components [[

]]

Steam Dryer Component	EPU	
	Peak Alternating Stress Intensity [[ ]] (psi)	Alternating Stress Ratio (ASR)
[[		
		]]

However, some code versions up to the 2007 edition did not specify an E value for correction of stresses associated with high cycle fatigue. The load controlled nature of data used to develop the ASME fatigue curves could be reason for not providing E on high cycle fatigue curves. As discussed in Reference 39-2, the correction for the Young's Modulus at the high cycle end of the fatigue curve is not required. Since testing for high cycle fatigue is generally done under load control (i.e., using tension specimens where the stress is P/A or bending

where the stress is Mc/I) the stress is independent of E. The effect of temperature must be evaluated, but the mean data curve already includes tests over a range of temperatures up to 800°F; therefore, the fatigue curve already includes the effect of temperature. As a result of these testing methods, [[

]]. Therefore, NEDC-33824P Table 4.4-1 values are appropriate [[ ]] and all ASR values remain greater than 2.0.

d. In the [[

]]

Table 39-2: [[

]]

Component Name	Time Shift Load Case	Time Interval	LF Adjusted Stress	HF Adjusted Stress	Combined Adjusted Stress	Alternating Stress Ratio
[[						

Component Name	Time Shift Load Case	Time Interval	LF Adjusted Stress	HF Adjusted Stress	Combined Adjusted Stress	Alternating Stress Ratio
						]]

Note:

1. [[

]]

[[

]]

[[

]]

Figure 39-14a

[[

]]

Figure 39-14b

[[

]]

Figure 39-14c

[[

]]

Figure 39-15a

[[

]]

Figure 39-15b

[[

]]

Figure 39-15c

[[

]]

Figure 39-16a

[[

]]

Figure 39-16b

[[

]]

Figure 39-16c

[[

]]

Figure 39-17a

[[

]]

Figure 39-17b

[[

]]

Figure 39-17c

[[

]]

Figure 39-18a

[[

]]

Figure 39-18b

[[

]]

Figure 39-18c

[[

]]

Figure 39-19a

[[

]]

Figure 39-19b

[[

]]

Figure 39-19c

[[

]]

Figure 39-20a

[[

]]

Figure 39-20b

[[

]]

Figure 39-20c

[[

]]

Figure 39-21a

[[

]]

Figure 39-21b

[[

]]

Figure 39-21c

[[

]]

Figure 39-22a

[[

]]

Figure 39-22b

[[

]]

Figure 39-22c

[[

]]

Figure 39-23a

[[

]]

Figure 39-23b

[[

]]

Figure 39-23c

[[

]]

Figure 39-24a

[[

]]

Figure 39-24b

[[

]]

Figure 39-24c

References:

39-1. John M. Biggs, Introduction to Structural Dynamics, McGraw-Hill Book Companies, 1964.

39.2 An Examination of the Role of the Assumed Young's Modulus Value At the High Cycle End of ASME Code Fatigue Curve for Stainless Steels. Ranganath, Sampath and Mehta, Hardayal, S. Boston: Pressure Vessels & Piping Conference, 2015.

Changes to NEDC-33824P Revision 0 – BFN Steam Dryer Analysis Report (SDAR):

None

EMCB-RAI 40

To help ensure conservatism in the [[
]], provide histograms of the summed BFN RSD loading [[ ]], along with histograms of the [[ ]] Also, provide histograms of the summed benchmark BWR/4 dryer loading, along with histograms of the simulated and measured on-dryer strains. Finally, provide histograms of the measured strains on the outer hood of the lead-in BFN RSD at EPU and include it in the 90-day EPU report. Provide a comparison of these histograms with those for Grand Gulf Nuclear Station, [[ ]] that were submitted earlier.

GEH Response

The conservatism of the chosen time segments is ensured through:

1. [[

]] As can be seen in Figures 4.1-14 and 4.1-15 of NEDC-33824P, [[

]]. Figures 4.1-14 and 4.1-15 provide the information being requested in the first sentence of this Request for Additional Information (RAI).

Specifically, these plots show the information for the spectral content for [[

]]

As discussed in NEDC-33824P, Figure 4.1-14 and Figure 4.1-15 show, respectively, the summed differential pressure ([[ ]]) per frequency band of the [[

]] The pressure load for these segments is approximately at, or above, average pressure for all significant frequency bands. The selected time is close to [[ ]]. As discussed in Step 5 of Section 4.1.2.2, it is practically [[

]] Each of the [[ ]] terms is applied to the [[

]]. This process provides the basic analysis [[ ]] bias and uncertainty corrections.

[[ ]] terms are included in the final stress adjustment (Section 4.2.5).

- [[

]]

The summed benchmark for the dryer loads for the BWR/4 pressure sensors compared to the measured are shown in Figure 3.2-8 (Upper Dryer) and Figure 3.2-9 (Lower Dryer) of NEDC-33824P Appendix C. The blue bar is the projected and red is the measured. This data [[

]] However, this frequency range is not over-predicted for the lower dryer. Specifically, the [[

]]

In order to understand if the [[

]] These are shown in NEDC-33824P Appendix C (Figures C4-1 to C4-10). It should be noted that [[ ]]. These sensors do not show any under-prediction in the [[

]]

It should be noted that the predicted stresses for BFN have the following additional adjustments:

1. [[

]]

The [[ ]]
These will be compared [[
]], including the [[ ]] applications.

Table 40-1. Summary of Locations for Requested Histogram Data

Requested Graphs	Location of Graphs	Summary of Display
[[		
		]]

Changes to NEDC-33824P Revision 0 – BFN Steam Dryer Analysis Report (SDAR):

NEDC-33824P Appendix C Revision 0: [[
]]

EMCB-RAI 41

In Section 6.5 of NEDC-33824P, Revision 0, the licensee discusses projecting [[ ]]. If the projected loading leads to acceptance limit violations, Section 6.6.1 states that [[

]] Substantiate using [[ ]] to trend SRV loads that are highly nonlinear using examples from previous SRV resonance trending in other plants. Also, demonstrate with an example how SRV resonance loads will be trended (also at intermediate power hold points) using the method described in Section 6.6.1.

GEH Response

As described in Section 6.5, during the [[

]]. If the [[ ]] indicate that there is not adequate [[ ]] to the [[ ]] to proceed with the power ascension, then the [[ ]]. In Section 6.6.1, the updated [[

]] provides assurance that [[

]] process described in NEDC-33824P Appendix E was [[ ]] replacement steam dryer. During this power ascension, the [[ ]] was used. Once the [[ ]]. Also, the [[ ]] did not exceed [[ ]], validating the process.

The [[ ]] that was used as the basis for the [[ ]] load will be used to illustrate the [[ ]] for the [[ ]]. As shown in NEDC-33824P, Figure 4.1-42, the [[ ]] once the [[ ]] has been established.

Figure 41-1 and Figure 41-2 below illustrate [[ ]] loading for the upper and lower dryer regions, respectively. The data in Figure 41-1 and Figure 41-2 are from Figure 4.1-44 of NEDC-33824P. Note that Figure 4.1-42 and 4.1-44 use the same [[ ]]; however, Figure 4.1-44 is corrected for the [[ ]], and the data is interpolated to remove the [[ ]] due to measurement at the power level hold points.

Figure 41-1 and Figure 41-2 show the [[

]] projections. As can be seen in the figures, the [[
]] The [[
]] is adequate for the test steps immediately following [[
]] because the available [[

]] is conservative when the [[
]].

[[
]] bounds the [[ ]] measured pressure curve at the higher power levels. This provides assurance that the [[

]]

[[

]]

Figure 41-1. [[

]]

[[

]]

Figure 41-2. [[

]]

Changes to NEDC-33824P Revision 0 – BFN Steam Dryer Analysis Report (SDAR):

None

EMCB-RAI 42

In NEDC-33824P, Appendix E (Reference 11), page E-11, GEH states in the Power Ascension Test Plan that power levels will be chosen [[
]]. What test conditions will be evaluated that [[

]] may be assessed. Provide core flow sweep test results at EPU conditions to the NRC shortly after the test. The core flow sweep test results are also to be included in the 90-day steam dryer EPU report.

GEH Response

See the response to EMCB-RAI 32 for a discussion [[
]]; the power levels of the signals will most likely sum.

The on-dryer instrumentation and Main Steam Line (MSL) data will be processed into the frequency domain. Outputs from the plant data will verify the Vane Passing Frequency (VPF) signal frequency. Power summed over the bandwidth [[

]]. If the sum of this same bandwidth between power levels is approximately equal, [[ ]] If the power summations are different than expected [[

]]

The Power Ascension Test Plan (PATP, NEDC-33824P, Appendix E, Section 3.2) for the instrumented dryer includes a test series where the power is held constant and the core flow varied over the licensed core flow operating range to measure [[

]]. This is included and stated in NEDC-33824P, Appendix E, Section 2.0, Item 4, page E-9; Section 2.0, Item 3, page E-10; and Section 3.2.

[[

]]

The licensee will provide the core flow sweep test results at [[ ]] to the Nuclear Regulatory Commission (NRC) “shortly” after the test, allowing time for processing, analysis

and verification. The [[ ]] test results will be included in the 90-day steam dryer [[ ]] report.

Changes to NEDC-33824P Revision 0 – BFN Steam Dryer Analysis Report (SDAR):

The sentence below will be added to NEDC-33824P, Appendix E, Section 3.2, before the last sentence in the last paragraph:

"In addition, data will be taken at the conditions where [[

]]"

EMCB-RAI 43

Provide a quantitative justification that ANSYS shell elements used to model the steam dryer in the finite element structural analysis of the steam dryer adequately capture peak stresses.

GEH Response

In ANSYS Version 14.0 (Reference 43-1), SHELL181 is the recommended four-node structural shell element for modeling thin to moderately-thick shell structures. The SHELL181 element formulation assumes the transverse shear is a parabolic distribution through the thickness (i.e., zero transverse shear stress at the top and bottom fibers and maximum at middle fiber). The ANSYS SHELL63 element type is a legacy element type in Version 14.0. It is formulated for analyzing relatively thin shell structures where transverse shear stiffness is negligible with respect to the in-plane stiffness. The ANSYS SHELL43 element type is also a legacy element type in Version 14.0. The SHELL43 element formulation assumes a uniform transverse shear distribution through the plate thickness and is well-suited for modeling thin to moderately thick structures. Both SHELL43 and SHELL63 element types are undocumented; however, these elements are [[ ]]. The Replacement Steam Dryer (RSD) Finite Element Model (FEM) [[ ]]. The reason for this choice is [[

]]

To determine the consequence of the transverse shear assumption in the ANSYS element formulation for the three element types, SHELL181, SHELL63, and SHELL43, a simplified study using the ANSYS verification manual test case VM39 (Reference 43-1) was performed. This test case uses a 10° sector of a circular plate with a center hole to study the differences between the three element types (see Figure 43-1). The plate thickness for the study is 0.25 inches and the inner (b) and outer (a) radii are 10 inches and 30 inches, respectively. For the material, the elastic modulus is 30 MSI and Poisson's ratio is 0.3. Symmetric boundary condition configurations are applied along the two radial edges with the inner diameter constrained in all six degrees of freedom. In order to test the transverse shear effect, the loading is modified as a total 4 lb. vertical force applied evenly at outer edge two nodes (Nodes 7 and 17) of the 10° sector as shown in Figure 43-1. This simplified test case configuration is similar to the [[ ]].

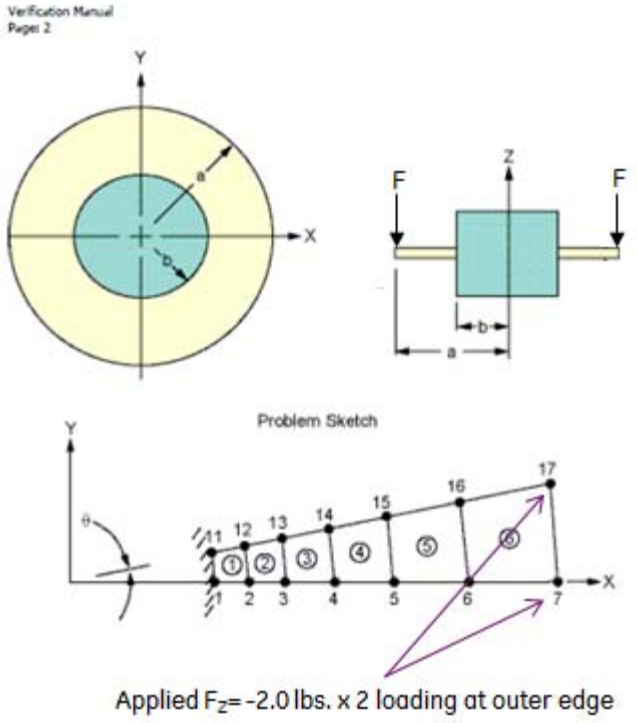

Figure 43-1. Finite Element Model Description for Test Case VM39 with Vertical Force Applied

Table 43-1 shows comparisons of the outer edge deflection and the element component stress SX in X (~ radial) direction for the inner diameter (Element 1) and outer diameter (Element 6) elements using the SHELL181 (ANSYS recommended element type) results as a base reference. The comparisons show the differences to be insignificant. However, the SHELL43 results are virtually identical to the SHELL181 results for the case analyzed.

To further illustrate the ANSYS transverse shear stress assumption for the three element types, Figures 43-2 to 43-4 provide the component stress listing at each node for Element 1 for the SHELL63, SHELL181 and SHELL43 element types, respectively. The results indicate that although there is no significant difference for the dominant in-plane stresses (SX and SY); the non-zero transverse shear stresses (SXZ and SYZ) are computed for SHELL181 and SHELL43 element types and not for the SHELL63 element type. Noting that the listed output contains three sets of data for the top, bottom, and middle fibers respectively, the SHELL181 top and bottom fibers assume a zero transverse shear stress with a maximum transverse shear stress in the middle fiber, while the SHELL43 element type assumes the transverse shear stress to be distributed uniformly throughout the thickness. Therefore, to adequately model locations where the transverse shear effect cannot be neglected, the SHELL181 or SHELL43 element types are recommended.

Table 43-1. Results Obtained from SHELL63, SHELL181 and SHELL43

	SHELL181	SHELL63	SHELL43	Percent Difference (63-181)/181	Percent Difference (43-181)/181
Deflection at Outer Edge (in)	-0.05755	-0.05850	-0.05757	1.6422%	0.0201%
SX Stress in Element 1 (psi)	2449.00	2424.04	2449.01	-1.0194%	0.0002%
SX Stress in Element 6 (psi)	168.06	177.02	168.06	5.3263%	-0.0001%

```
PRINT S    ELEMENT SOLUTION PER ELEMENT

***** POST1 ELEMENT NODAL STRESS LISTING *****

 LOAD STEP=     1  SUBSTEP=     1
  TIME=    1.0000      LOAD CASE=   0
 SHELL RESULTS FOR TOP/BOTTOM ALSO MID WHERE APPROPRIATE

 THE FOLLOWING X,Y,Z VALUES ARE IN GLOBAL COORDINATES


 ELEMENT=       1        SHELL63
   NODE     SX          SY          SZ          SXY         SYZ         SXZ
      1    2525.4      749.11      0.0000     -16.783      0.0000      0.0000
      2    2373.1      1040.2      0.0000     -3.6686      0.0000      0.0000
     12    2341.5      1086.6      0.0000      233.04      0.0000      0.0000
     11    2456.2      803.78      0.0000      318.99      0.0000      0.0000
      1   -2525.4     -749.11      0.0000      16.783      0.0000      0.0000
      2   -2373.1     -1040.2      0.0000      3.6686      0.0000      0.0000
     12   -2341.5     -1086.6      0.0000     -233.04      0.0000      0.0000
     11   -2456.2     -803.78      0.0000     -318.99      0.0000      0.0000
      1    0.0000      0.0000      0.0000      0.0000      0.0000      0.0000
      2    0.0000      0.0000      0.0000      0.0000      0.0000      0.0000
     12    0.0000      0.0000      0.0000      0.0000      0.0000      0.0000
     11    0.0000      0.0000      0.0000      0.0000      0.0000      0.0000
```

Figure 43-2. Element Component Stresses (psi) for Element #1 Using SHELL63

PRINT S ELEMENT SOLUTION PER ELEMENT

***** POST1 ELEMENT NODAL STRESS LISTING *****

LOAD STEP= 1 SUBSTEP= 1
TIME= 1.0000 LOAD CASE= 0
SHELL RESULTS FOR TOP/BOTTOM ALSO MID WHERE APPROPRIATE

THE FOLLOWING X,Y,Z VALUES ARE IN GLOBAL COORDINATES

ELEMENT= 1 SHELL181

NODE	SX	SY	SZ	SXY	SYZ	SXZ
1	2406.1	731.74	0.0000	73.244	0.0000	0.0000
2	2515.3	1095.9	0.0000	62.137	0.0000	0.0000
12	2493.9	1117.5	0.0000	184.45	0.0000	0.0000
11	2380.8	757.22	0.0000	217.52	0.0000	0.0000
1	-2406.1	-731.74	0.0000	-73.244	0.0000	0.0000
2	-2515.3	-1095.9	0.0000	-62.137	0.0000	0.0000
12	-2493.9	-1117.5	0.0000	-184.45	0.0000	0.0000
11	-2380.8	-757.22	0.0000	-217.52	0.0000	0.0000
1	0.0000	0.0000	0.0000	0.0000	-1.0900	-12.459
2	0.0000	0.0000	0.0000	0.0000	-1.7399	-12.368
12	0.0000	0.0000	0.0000	0.0000	-1.7708	-12.721
11	0.0000	0.0000	0.0000	0.0000	-1.1209	-12.812

Figure 43-3. Element Component Stresses (psi) for Element #1 Using SHELL181

PRINT S ELEMENT SOLUTION PER ELEMENT

***** POST1 ELEMENT NODAL STRESS LISTING *****

LOAD STEP= 1 SUBSTEP= 1
TIME= 1.0000 LOAD CASE= 0
SHELL RESULTS FOR TOP/BOTTOM ALSO MID WHERE APPROPRIATE

THE FOLLOWING X,Y,Z VALUES ARE IN GLOBAL COORDINATES

ELEMENT= 1 SHELL43

NODE	SX	SY	SZ	SXY	SYZ	SXZ
1	2406.1	731.76	0.0000	73.245	-0.73410	-8.3908
2	2515.4	1095.9	0.0000	62.096	-0.73410	-8.3908
12	2493.8	1117.4	0.0000	184.40	-0.73410	-8.3908
11	2380.7	757.20	0.0000	217.51	-0.73410	-8.3908
1	-2406.1	-731.76	0.0000	-73.245	-0.73410	-8.3908
2	-2515.4	-1095.9	0.0000	-62.096	-0.73410	-8.3908
12	-2493.8	-1117.4	0.0000	-184.40	-0.73410	-8.3908
11	-2380.7	-757.20	0.0000	-217.51	-0.73410	-8.3908

Figure 43-4. Element Component Stresses (psi) for Element #1 Using SHELL43

During the RSD FEM development, two FIV full transient dynamic analysis test runs were performed using a [[

]]

Although SHELL181 is the ANSYS recommended element type, the VM39 case study shows that the SHELL43 element type and SHELL181 element type calculate approximately the same result. Table 43-2 presents the comparison of the [[

]] as taken from Table 4.4-1 of NEDC-33824P Revision 0. [[

]]; therefore, the results for these

components are not applicable to this Request for Additional Information (RAI) response. The results show that [[

]]

The final version of the Browns Ferry Nuclear Plant (BFN) RSD FEM is primarily comprised of ANSYS [[

]]

Table 43-2

[[			

]]

Reference:

43-1. ANSYS Help Documentation Release 14.0 SAS IP, Inc.

Changes to NEDC-33824P Revision 0 – BFN Steam Dryer Analysis Report (SDAR):

None

ENCLOSURE 3

General Electric Hitachi Affidavit

GE-Hitachi Nuclear Energy Americas LLC

AFFIDAVIT

I, Lisa K. Schichlein, state as follows:

(1) I am a Senior Project Manager, NPP/Services Licensing, Regulatory Affairs, GE-Hitachi Nuclear Energy Americas LLC (GEH), and have been delegated the function of reviewing the information described in paragraph (2) which is sought to be withheld, and have been authorized to apply for its withholding.

(2) The information sought to be withheld is contained in Enclosure 1 of GEH letter 175528-019, "Second Set of GEH RAI Responses in Support of the Browns Ferry Steam Dryer Replacement," dated July 22, 2016. The GEH proprietary information in Enclosure 1, which is entitled "GEH Response to EMCB RAIs in Support of TVA Browns Ferry Replacement Steam Dryer," is identified by a dotted underline inside double square brackets. [[This sentence is an example.{3}]] Figures and large objects are identified with double square brackets before and after the object. In each case, the superscript notation {3} refers to Paragraph (3) of this affidavit, which provides the basis for the proprietary determination.

(3) In making this application for withholding of proprietary information of which it is the owner or licensee, GEH relies upon the exemption from disclosure set forth in the *Freedom of Information Act* ("FOIA"), 5 U.S.C. Sec. 552(b)(4), and the *Trade Secrets Act*, 18 U.S.C. Sec. 1905, and NRC regulations 10 CFR 9.17(a)(4), and 2.390(a)(4) for trade secrets (Exemption 4). The material for which exemption from disclosure is here sought also qualifies under the narrower definition of trade secret, within the meanings assigned to those terms for purposes of FOIA Exemption 4 in, respectively, Critical Mass Energy Project v. Nuclear Regulatory Commission, 975 F.2d 871 (D.C. Cir. 1992), and Public Citizen Health Research Group v. FDA, 704 F.2d 1280 (D.C. Cir. 1983).

(4) The information sought to be withheld is considered to be proprietary for the reasons set forth in paragraphs (4)a. and (4)b. Some examples of categories of information that fit into the definition of proprietary information are:

a. Information that discloses a process, method, or apparatus, including supporting data and analyses, where prevention of its use by GEH's competitors without license from GEH constitutes a competitive economic advantage over other companies;

b. Information that, if used by a competitor, would reduce their expenditure of resources or improve their competitive position in the design, manufacture, shipment, installation, assurance of quality, or licensing of a similar product;

c. Information that reveals aspects of past, present, or future GEH customer-funded development plans and programs, resulting in potential products to GEH;

d. Information that discloses trade secret or potentially patentable subject matter for which it may be desirable to obtain patent protection.

(5) To address 10 CFR 2.390(b)(4), the information sought to be withheld is being submitted to NRC in confidence. The information is of a sort customarily held in confidence by GEH, and is in fact so held. The information sought to be withheld has, to the best of my knowledge and belief, consistently been held in confidence by GEH, not been disclosed publicly, and not been made available in public sources. All disclosures to third parties, including any required transmittals to the NRC, have been made, or must be made, pursuant to regulatory provisions or proprietary or confidentiality agreements that provide for maintaining the information in confidence. The initial designation of this information as proprietary information, and the subsequent steps taken to prevent its unauthorized disclosure, are as set forth in the following paragraphs (6) and (7).

(6) Initial approval of proprietary treatment of a document is made by the manager of the originating component, who is the person most likely to be acquainted with the value and sensitivity of the information in relation to industry knowledge, or who is the person most likely to be subject to the terms under which it was licensed to GEH.

(7) The procedure for approval of external release of such a document typically requires review by the staff manager, project manager, principal scientist, or other equivalent authority for technical content, competitive effect, and determination of the accuracy of the proprietary designation. Disclosures outside GEH are limited to regulatory bodies, customers, and potential customers, and their agents, suppliers, and licensees, and others with a legitimate need for the information, and then only in accordance with appropriate regulatory provisions or proprietary or confidentiality agreements.

(8) The information identified in paragraph (2), above, is classified as proprietary because it contains detailed GEH design information of the methodology used in the design and analysis of the steam dryers for the GEH Boiling Water Reactor (BWR). Development of these methods, techniques, and information and their application for the design, modification, and analyses methodologies and processes was achieved at a significant cost to GEH.

The development of the evaluation processes along with the interpretation and application of the analytical results is derived from the extensive experience and information databases that constitute a major GEH asset.

(9) Public disclosure of the information sought to be withheld is likely to cause substantial harm to GEH's competitive position and foreclose or reduce the availability of profit-making opportunities. The information is part of GEH's comprehensive BWR safety and technology base, and its commercial value extends beyond the original development cost. The value of the technology base goes beyond the extensive physical database and analytical methodology and includes development of the expertise to determine and apply

the appropriate evaluation process. In addition, the technology base includes the value derived from providing analyses done with NRC-approved methods.

The research, development, engineering, analytical and NRC review costs comprise a substantial investment of time and money by GEH. The precise value of the expertise to devise an evaluation process and apply the correct analytical methodology is difficult to quantify, but it clearly is substantial. GEH's competitive advantage will be lost if its competitors are able to use the results of the GEH experience to normalize or verify their own process or if they are able to claim an equivalent understanding by demonstrating that they can arrive at the same or similar conclusions.

The value of this information to GEH would be lost if the information were disclosed to the public. Making such information available to competitors without their having been required to undertake a similar expenditure of resources would unfairly provide competitors with a windfall, and deprive GEH of the opportunity to exercise its competitive advantage to seek an adequate return on its large investment in developing and obtaining these very valuable analytical tools.

I declare under penalty of perjury that the foregoing is true and correct.

Executed on this 22nd day of July 2016.

Lisa K. Schichlein
Senior Project Manager, NPP/Services Licensing
Regulatory Affairs
GE-Hitachi Nuclear Energy Americas LLC
3901 Castle Hayne Road
Wilmington, NC 28401
Lisa.Schichlein@ge.com